NIH Public Access
Author Manuscript
Cancer Res. Author manuscript; available in PMC 2013 November 01.

Published in final edited form as:
Cancer Res. 2012 November 1; 72(21): 5566–5575. doi:10.1158/0008-5472.CAN-12-1683.

Overcoming limitations in nanoparticle drug delivery: triggered, intravascular release to improve drug penetration into tumors

Ashley A. Manzoor[*,1,2], **Lars H. Lindner**[*,4,5,6], **Chelsea D. Landon**[2], **Ji-Young Park**[2], **Andrew J. Simnick**[3], **Matthew R. Dreher**[7], **Shiva Das**[1,2], **Gabi Hanna**[2], **Won Park**[2], **Ashutosh Chilkoti**[3], **Gerben A. Koning**[4], **Timo L.M. ten Hagen**[4], **David Needham**[3], and **Mark W. Dewhirst**[1,2,3]

[1]Medical Physics Program, Duke University, Durham, North Carolina [2]Department of Radiation Oncology, Duke University Medical Center, Durham, North Carolina [3]Department of Biomedical Engineering, Duke University, Durham, North Carolina [4]Laboratory Experimental Surgical Oncology, Section Surgical Oncology, Department of Surgery, Erasmus Medical Center, Rotterdam, The Netherlands [5]Department of Internal Medicine III, University Hospital Grosshadern, Ludwig-Maximilians University, Munich, Germany [6]CCG Hyperthermia, Helmholtz Zentrum Munchen, German Research Center for Environmental Health, Munich, Germany [7]Radiology and Imaging Sciences, Clinical Center, National Institutes of Health, Bethesda, Maryland

Abstract

Traditionally, the goal of nanoparticle-based chemotherapy has been to decrease normal tissue toxicity by improving drug specificity to tumors. The EPR effect (Enhanced Permeability and Retention) can permit passive accumulation into tumor interstitium. However, suboptimal delivery is achieved with most nanoparticles because of heterogeneities of vascular permeability, which limits nanoparticle penetration. Further, slow drug release limits bioavailability. We developed a fast drug-releasing liposome triggered by local heat that has already shown substantial anti-tumor efficacy and is in human trials. Here, we demonstrate that thermally sensitive liposomes release doxorubicin inside the tumor vasculature. Real-time confocal imaging of doxorubicin delivery to murine tumors in window chambers and histologic analysis of flank tumors illustrates that intravascular drug release increases free drug in the interstitial space. This increases both the time that tumor cells are exposed to maximum drug levels and the drug penetration distance, compared with free drug or traditional pegylated liposomes. These improvements in drug bioavailability establish a new paradigm in drug delivery: rapidly triggered drug release in the tumor bloodstream.

Keywords

temperature-sensitive liposome; hyperthermia; nanoparticle

[*]These authors contributed equally to this work

Conflict of Interest Statement: Dr. Needham is the inventor of Dox-TSL. Dox-TSL was licensed from Duke University by Celsion Coporation. Drs. Dewhirst and Needham are former consultants for Celsion and Dr. Dewhirst owns stock in the company. None of the other authors have a conflict.

$watermark-text
$watermark-text
$watermark-text

$watermark-text

$watermark-text

$watermark-text

Introduction

A major challenge in chemotherapy is to change the biodistribution of drugs to reduce free drug toxicity and favor tumor accumulation. Attempts to overcome this challenge have focused on nanoparticles, such as liposomes (1) (2) and other self-assembling systems (3, 4) (5). The hyperpermeability of tumor vasculature led to the hypothesis that liposomes and other particles could accumulate more specifically in tumor tissue than normal tissue by passive extravasation; the process was termed the enhanced permeability and retention (EPR) effect (6, 7). As an extension, additional tumor specificity could be achieved with active ligand targeting. While these methods have been shown to increase the amount of drug delivered, there is growing evidence (6, 8-10) that many nanoparticle delivery systems are too large to extravasate in human tumors. Even when tumor vasculature is permeable to 100nm liposomes, the distribution pattern is extremely heterogeneous and susceptible to large inter- and intratumoral variances in vascular permeability and ligand expression (9, 11). Further, the relatively large size of nanoparticles limits their penetration depth to 1-2 cell layers from blood vessels (6, 8-10, 12).

Nanoparticles also release drug slowly; thus, tumor cells may not be exposed to concentrations high enough to result in cell death (9, 13). Consequently, a gap exists between shielding normal tissue from drug and delivering the drug at therapeutic concentrations to all tumor cells. One solution would be to initiate local drug release from a nanoparticle in the tumor's bloodstream, where it can diffuse into the tissue, down its concentration gradient. This would avoid the reliance on particle extravasation.

We developed thermally sensitive liposomes (Dox-TSLs) that rapidly release doxorubicin in response to 40-42°C heat (14-20). Preclinical work demonstrated tumor drug levels up to 30 times higher than free drug and 3-5 times greater than traditional liposomes; the enhanced delivery was linked to superior anti-tumor efficacy (15, 21). Interestingly, timing of liposome injection vs. application of hyperthermia altered anti-tumor efficacy in rat fibrosarcomas (22). When Dox-TSLs were administered after tumors were preheated, tumor drug concentrations were doubled compared to Dox-TSL administration prior to hyperthermia. We speculated the increased drug delivery in the first case was due to intravascular release during peak plasma concentrations of liposomal drug.

This result led to the current hypothesis: *The mechanism of drug delivery from Dox-TSL + heat is due to perivascular drug penetration as a result of rapidly triggered intravascular liposomal drug release*. This method maintains the toxicity benefits of sequestering drug until it reaches the tumor where it releases drug with a localized trigger. Intravascular release from TSLs overcomes heterogeneity in vascular permeability and limited penetration associated with the EPR effect. In this context, TSLs serve as a continuous intravascular infusion of drug which originates at the tumor site. This creates high intravascular drug concentrations that drive drug uptake by cells and increase drug penetration further from vessels.

While the intravascular release hypothesis has existed since the early work on TSLs in the 1970's (23-25), it has not been shown *in vivo*; the enhancement in drug delivery has only been demonstrated by an increase in overall tumor drug concentrations, not drug penetration. Herein we present the first *in vivo* evidence of intravascular drug release using intravital confocal microscopy and illustrate that intravascular drug release improves drug penetration to reach more tumor cells than either the EPR effect with pegylated liposomes or with free drug.

$watermark-text

$watermark-text

$watermark-text

Materials and Methods

Cell lines

Human squamous cell carcinoma (FaDu) cells were grown as monolayers in tissue culture flasks containing minimal essential DMEM supplemented with 10% heat-inactivated FBS, penicillin and streptomycin (Gibco, Carlsbad, CA). Cell cultures were kept at 37°C with 5% CO_2 in air. B16BL6 melanomas were transplanted to window chambers from donor animals. Both cell lines were obtained from the ATCC.

Dorsal Skin Fold Window Chamber

All animal experiments were performed in accordance with Duke University or Erasmus Medical Center's institutional animal care and use committee guidelines. Either nude athymic mice (FaDu tumor model) or eNOS-GFP transgenic mice (B16BL6 melanoma model) were used. The eNOS-GFP transgenic mouse model contains the eNOS-GFP fusion protein expression, restricted to the endothelial cells. Mice were anesthetized and then underwent dorsal window chamber implantation as described previously (26). Additional details are in Supplemental Materials and Methods.

Liposome Preparation

This study utilized two different liposome formulations, the primary TSL formulation, used for evaluating drug kinetics and penetration, and a second formulation prepared in Rotterdam, Netherlands to corroborate intravascular release of drug in eNOS-GFP mice. The first liposome preparation consisted of 99.9mol% of DPPC, MSPC, and DSPE-PEG2000 with corresponding mole percentages of 85:9.8:5.2, along with 0.5mol% fluorescein DHPE. TSLs were similarly prepared at the Erasmus Medical Center, Netherlands, but with the mole percentages 90:10:4 (DPPC:MSPC:DSPE-PEG2000). Doxorubicin loading was achieved by the remote pH gradient method (27). Further details are provided in Supplemental Methods.

Confocal Image Acquisition

Nude mice with dorsal window chambers were anesthetized (Nembutal; 85mg/kg i.p.) and positioned on a custom-designed microscope stage and heating device for localized heating to the window chamber between 40.7-41.8°C (or 34–36°C in unheated controls) (12). Core body temperature was maintained with a warming pad set at 37°C. The tail vein was cannulated and 0.1mL of 10mg/mL 2-MDa Rhodamine-labeled Dextran (Molecular Probes, Eugene, Oregon) was injected i.v. A z-stack of images was collected with a LSM 510 laser-scanning confocal microscope (Zeiss, Jena, Germany) through approximately 50-100μm of tissue, using a 543 excitation laser and LP 560 emission filter. A plane approximately halfway through the z-stack image was chosen for continual sequential imaging of either doxorubicin and dextran (when free doxorubicin was injected) or doxorubicin and fluorescein-labeled liposomes (when Dox-TSL was injected); both at 6mg/kg. Images were obtained every 5sec for 20min, including 20sec of background images. Four treatment groups were evaluated: doxorubicin +heat (n=5), doxorubicin -heat (n=5), Dox-TSL +heat (n=6) and Dox-TSL - heat (n=4).

For visualization of the intravascular doxorubicin release in the eNOS-GFP mice, animals were anesthetized with isofluorane (Nicholas Piramal (I) Limited, London, UK) and placed on a thermal stage at 37°C. Heating of the chamber to target tumor temperatures of 41°C was accomplished by an external circular resistive electric heating coil attached to the glass of the back side of a glass coverslip (28). The doxorubicin dose was 5mg/kg. Representative pictures out of 4 independent experiments applying Dox-TSL+heat are shown. Additional details are provided in Supplemental Methods.

$watermark-text

$watermark-text

$watermark-text

Confocal Image Analysis

Data were preprocessed to segment vascular and extravascular spaces, and doxorubicin fluorescence was normalized and corrected for bleed-through. Additional analysis details are provided in Supplemental Methods. Drug penetration depth was determined by converting the 3D vascular mask from the rhodamine-dextran images into a distance map that related the distance of each pixel from the nearest vascular structure in 3D space. A distance of zero corresponded to the end of the intervascular space. Boundary effects were removed by truncating the dataset by 50 pixels on all sides in the x-y plane. Fluorescence intensities for pixels located at each distance from the nearest vessel were then averaged.

Histology Image Analysis

Athymic nude mice were injected with 1×10^6 FaDu cells into the right leg. Tumors were 8–12mm in diameter when used (ulcerated tumors excluded) in four treatment groups: Dox-TSL +heat (n=9), Dox with (n=7) and without heat (n=5), and Doxil™ +heat (n=8). Mice were anesthetized (85mg/kg Nembutal i.p.) and fitted with a tail vein catheter and a rectal temperature monitoring probe to measure core body temperature during water bath heating (see Supplemental Methods).

Tumor-bearing legs were preheated for 10min prior to injection to reach thermal steady state. Mice were then injected i.v. with 15mg/kg Dox-TSL, free doxorubicin, or Doxil™ at 2mg/mL to ensure an injected volume per mouse less than 0.2mL. Following injection, the animals were heated for an additional 20min, then removed and allowed to cool for 10min prior to sacrifice (Doxil™ animals sacrificed 24hr post-treatment). Tumors were snap frozen over liquid Nitrogen.

Entire tumor sections were imaged for doxorubicin and stained and imaged for CD31 using a Zeiss Axioscope 2 scanning stage with 20× objective and Metamorph image software (see Supplemental Methods).

Statistical Analysis

Data are presented as means with standard deviations. Statistical differences between groups were computed using the Wilcoxon rank-sum test. $AUC_{0\text{-}20}$ values are expressed as median ± standard deviations of the product $\%I_{vasc,max} \times$ seconds.

Results

Drug delivery through intravascular release

Free drug administration was compared with intravascular release of drug from Dox-TSL. Heat demonstrated little influence on the accumulation of free doxorubicin (red signal), which diffused out of the vascular space (green signal) and into the extravascular space immediately after injection (Fig 1 and Supplemental Movies 1 and 2). However, declining vascular concentration caused the blood vessel compartment to switch from a drug source to a drug sink, resulting in reabsorption of drug into the vasculature more quickly than it can diffuse and enter cells. This leads to limited tumor cell exposure. Thus, extravascular drug levels quickly declined, with a precipitous drop in apparent drug accumulation within 5min of injection, in line with previous observations (13, 29). In Figure 1, free drug reabsorption into the vasculature is reflected by a decrease in drug (shown in red) in the extravascular region. As the reabsorption occurs more slowly than the blood flow rate in the nearby vessels, any drug that is reabsorbed into the vascular compartment is immediately removed from the tumor area, explaining why the vessels do not appear to have more drug during reabsorption.

$watermark-text

$watermark-text

$watermark-text

Dox-TSL's prolonged plasma half-life maintains high intravascular concentrations, resulting in increased accumulation of drug with time in the interstitial space (Fig 1 and Supplemental Movies). In the absence of heat, doxorubicin remains contained within the liposome and confined to blood vessels. To investigate intravascular release, fluorescently-labeled liposomes were imaged to determine the contribution of extravasation versus intravascular release (Fig 2). Overlap between green lipid label and red fluorescence of doxorubicin is seen as yellow. The intravascular signal remains strongly yellow throughout the 20min, while the red signal increases in the interstitial space. In contrast, there is very little yellow color in the interstitial space during heating. The lack of overlap between lipid and doxorubicin fluorescence in the interstitial space proves that drug accumulation in the interstitial space is due to release from liposomes still confined in the bloodstream. Intravascular release of doxorubicin and subsequent redistribution into tumor tissue is further illustrated with B16 melanoma using the eNOS-GFPtg mouse model (Fig 3 and Supplemental movie 2).

Enhanced tumor tissue uptake of drug

For each method of drug delivery, vascular clearance and extravascular accumulation of drug were quantified with image analysis (Fig 4). Intravascular release results in longer tumor cell exposure at higher drug concentrations compared to free drug. Free drug administration, ± heat, results in peak extravascular drug levels within 1min. Thereafter, drug levels in the interstitial space declines as vascular concentration falls. The drop in vascular concentration is a reflection of elimination and distribution of drug to other organs. Within 20min, residual drug levels in tumor were reduced to 9.6% +/- 2.0% of the original peak intravascular drug levels ($I_{vasc,max}$) in heated tumors and 13.7% +/- 5.7% in non-heated tumors. In contrast, the high intravascular drug levels maintained by the rapidly-releasing liposomes allow for sustained drug accumulation in the extravascular space. At 20min, drug is continuing to accumulate, with extravascular levels at 160% +/- 47% of the peak vascular drug level, 11-17-fold higher than free drug.

The area under the concentration-time curve (AUC) for the extravascular space provides a measure of the cumulative exposure of tumor cells to drug (12, 13). Within the first 20min, AUC_{0-20} values of free drug with and without heat are not statistically different, 156.8 +/- 41.7 and 185.2 +/- 160.8, respectively (p-value=0.6905). The AUC_{0-20} value for heated nanoparticles was 9-fold higher than free drug +heat, 1700 +/- 863.1 (p-value=0.0317). After the 20min heating, the AUC value for the Dox-TSL treatment group was still increasing due to continual accumulation of drug, while AUC increases in the free drug +heat group with each additional minute are minimal due to very low intravascular drug levels. This AUC_{0-20} value is only indicative of the first 20min of drug delivery during a typical 1hr heat treatment. Thus, these differences would be magnified for a 1hr exposure. The ability to maximize gains in AUC will be dependent on the local liposome concentration in the blood supply, underscoring the importance of heating prior to liposome injection. Starting heat after liposome injection would be expected to result in suboptimal AUC, due to declining vascular levels of Dox-TSL caused by clearance from the bloodstream (30). Maximum AUC could also be affected by the circulation kinetics and stability of the TSL formulation in plasma.

Enhanced drug penetration

Doxorubicin's poor penetration characteristics have been highlighted *in vivo* with mouse studies and in breast cancer patients (31, 32). To determine if intravascular release resulted in enhanced drug penetration in addition to accumulation, we first used image analysis to quantify relative drug concentrations with distance away from blood vessels (Fig 5). Administration of free drug exhibits a characteristic decline in drug concentration with

$watermark-text

$watermark-text

$watermark-text

distance from vessels; falling intravascular concentrations quickly cause drug to diffuse back towards the vasculature, resulting in relatively low drug retention outside the microvessels. At distances of 35μm from vessels (3-4 cell layers), the maximum amount of drug delivered within the first few minutes was only 31% +/- 7% of the peak intravascular drug level ($I_{vasc,max}$), and at 20min after injection, the amount of drug remaining at this distance declined to 10% +/- 2%. Drug penetration for free drug without heat was similar, 28% +/- 5% at maximum and 14% +/- 4% at 20min.

Drug delivered with heat-triggered liposomes was continuous throughout the period of heating, resulting in increased levels of drug out to 35μm. This penetration was the furthest possible depth measureable in the window chambers, given the heterogeneity of vessels across all groups and tumor regions. In contrast to the 10% residual drug at 35μm from vessels after 20min with free drug, Dox-TSL drug levels at this same distance were 138% +/- 45% of $I_{vasc,max}$ (p-value=0.0087). Additionally, drug accumulation at the endothelial cell barrier appeared to exhibit saturation kinetics; the drug level present at the endothelial cell edge did increase, but to a lesser extent than at further distances from microvessels. Drug accumulation at the endothelial cell edge changed from 88% +/- 12% of $I_{vasc,max}$ at time 0 to 126% +/- 32% of $I_{vasc,max}$ at 20min. However, at distances 10μm from the vasculature, the increase was more dramatic, from 41% +/- 16% at time 0 to 180% +/- 46% at 20min. Thus, the sustained intravascular release of drug may aid in saturating endothelial and tumor cell drug transport mechanisms, providing a method to enhance perivascular penetration. Maintaining high intravascular drug levels led to extravascular drug concentrations that exceeded maximal plasma levels. This is most likely due to cellular uptake of the drug, which removes drug from the interstitial space, thus maintaining the concentration gradient. Indeed, nuclear accumulation of drug is readily seen in the confocal images and is consistent with our prior observation of increased DNA-bound drug for the Dox-TSL formulation, compared with free drug or non-thermally sensitive liposomes (15). This ability to locally deliver drug concentrations that exceed vascular concentrations cannot be achieved with free drugs or non-thermally sensitive pegylated liposomes, where the extravasation is dependent entirely upon pharmacodynamics and/or the EPR effect, respectively (8, 33, 34).

To further define the enhanced drug penetration from Dox-TSL, we performed histologic analysis of flank FaDu tumors on mice that were given Dox-TSL+heat, free drug ± heat, or Doxil™ +heat. Tumors were harvested 30min after heating for all treatment groups except the Doxil™ +heat group, which was harvested 24hr post-treatment in order to directly compare the Dox-TSL penetration distance with the maximum nanoparticle accumulation typically seen with the EPR effect (8, 33, 34). Tissue sections were imaged for the vascular marker CD31 and doxorubicin, and then analyzed using custom Matlab code to determine the median penetration distance of drug from vessels over the entire tumor section. With free drug, median drug penetration was 29 +/- 10 and 55 +/- 6μm, without and with heat, respectively (Fig 6), which is comparable to published reports for this drug (32). However, the concentration delivered at all distances with free drug was much lower than with either Dox-TSL or Doxil™, with maximum fluorescence of free drug being 16-25% of the maximum fluorescence closest to vessels with Dox-TSL. A direct comparison was also made between TSL+heat and the traditional liposome Doxil™ +heat. Dox-TSL+heat resulted in a penetration distance double that achievable with Doxil™ +heat; drug penetrated 78 +/- 18μm compared to 34 +/- 9μm, respectively (p-value=0.0106). Additionally, at the point where drug levels from Dox-TSL+heat started to fall below the level immediately proximal to the vasculature, drug levels had already declined to 36% of their initial value for the Doxil™ +heat group. Thus, the confocal and histology data together show that liposome-mediated intravascular drug release not only exposes tumor cells to a higher drug concentration for a longer time period, but also improves tumor

exposure to drug at every distance from vessels. Most importantly, the overall achievable drug penetration is doubled with intravascular release compared to free drug or the EPR effect seen with Doxil™ +heat.

Discussion

While traditional chemotherapeutic drugs like doxorubicin, cisplatin and paclitaxel have dose limiting toxicities, new *molecularly targeted cancer therapies* more specifically interfere with cancer cell proliferation and metastasis, and have the potential to be more effective and less harmful to normal cells. Yet, the challenge for these molecular therapeutic agents is still fundamentally the same – limited delivery. Lack of drug penetration or sufficient concentration to result in tumor toxicity has been highlighted using multiple small molecule chemotherapeutics (32, 35-37), and the newer fleet of monoclonal antibodies and small molecule inhibitors would be expected to display these same penetration-limited pharmacodynamics (12, 36). The larger the size of the drug, the more tumor penetration becomes a fundamental limitation. Lack of drug penetration becomes even more significant when using nanoparticles, as their perivascular accumulation and slow release pose a severe hindrance to drug delivery. The results here show that even with hyperthermia, the maximum penetration of Doxil™ is limited to 34μm; other studies not utilizing hyperthermia have reported even more limited penetration of 8-16μm (10).

Treatment with TSL+heat to local tumors can be thought of as the fusion of two traditional approaches to drug delivery: 1) continuous infusion of drug and 2) nanoparticle encapsulation. Drug infusions maintain elevated drug levels in the bloodstream and thus prevent drug washout from the tumor prior to cellular uptake (13). However, this approach does not provide any tumor selectivity. Alternatively, nanoparticles are typically designed to shield drug from normal tissue, but this strategy sacrifices drug bioavailability. Our results present the union of these two ideas – using a liposome to shield the normal tissue from toxicity, and incorporating local release in the tumor vascular supply, effectively serving as a continuous infusion that originates at the tumor site. While this idea was previously postulated for TSL (24, 25, 38), these results are the first *in vivo* evidence to prove that intravascular release is the predominant method of drug delivery. Further, these results show that this approach exposes tumor cells to drug over a longer time frame, delivers drug at a higher concentration at all distances from blood vessels, and doubles the maximum penetration distance of drug into tumor tissue. It is also important to note that the window chamber data for Dox-TSL+heat treatment clearly demonstrate that drug is being taken up into tumor cell nuclei for both tumor types studied. We previously showed that the percentage of DNA-bound doxorubicin with Dox-TSL is substantially greater than what can be achieved with a Doxil™-type of liposome formulation (15). The Doxil™ formulation is not thermally sensitive; we have shown that Doxil™ does not exhibit enhanced drug release in the mild hyperthermia temperature range (41-45°C) (16). Thus, we would not expect significant nuclear uptake of doxorubicin during heating with Doxil™. This recapitulates the concept that Dox-TSL intravascular drug release/delivery provides a venue for bioavailable drug delivery, as compared to Doxil™, where the drug remains entrapped inside the liposome after delivery, where subsequent release occurs over days to weeks.

Since the formulation and efficacy publications for Dox-TSL in 2000 (15, 16), several studies have been published, including additional preclinical studies (21, 22), a canine clinical trial (39), and pharmacokinetic data from a human clinical trial (30). A comprehensive review of these studies was recently published (40).

Dox-TSL has also been tested in three phase I clinical trials. Results of a phase I trial for patients with primary and metastatic tumors of the liver treated with the combination of

$watermark-text $watermark-text $watermark-text

$watermark-text

$watermark-text

$watermark-text

radiofrequency ablation (RFA) and Dox-TSL have been reported (41). This dose escalation study involved a 30min infusion of Dox-TSL given 15min prior to RFA. A statistically significant difference in the time to treatment failure was observed between the patients receiving at least the MTD and patients receiving less than the MTD (374 vs. 80 days, respectively). The authors concluded that the combination of RFA and Dox-TSL was safe and likely more efficacious than RFA alone. These results formed the rationale for a multi-national phase III trial for treatment of hepatocellular carcinoma (NCT00617981) (42). Accrual was recently completed and follow-up is in progress. A report of this trial is expected within the next year.

A phase I trial has been completed and a phase II trial has been initiated for the treatment of recurrent chest wall disease in breast cancer patients with the combination of Dox-TSL and hyperthermia (NCT00826085) (43). A prior phase I study was conducted at Duke University, and a manuscript combining these two studies is being prepared for submission. Due to the broad range of doxorubicin anti-tumor efficacy, Dox-TSL has the potential to be used to treat multiple other cancer types.

Further research into intravascular release methods will be dependent on the ability to localize the intended stimulus, in this instance, application of hyperthermia to the tumor. Advances in the application of hyperthermia over the last decade have already made this a clinical reality for localized tumors (44-46). This paper presents the idea of fast triggered release, which may not necessarily be limited to stimulus by hyperthermia, however. With further advances in nanoparticle technology, this same mechanism may equally be achieved using other trigger stimuli, including ultrasound, light, radiation, or potentially even magnetic fields. Further, the ability to deliver drug to tumor at vascular penetration distances twice as far as previously achievable may result in increased benefit from microenvironmentally-targeted drugs, such as hypoxic cytotoxins, which have shown dramatic *in vitro* results but often fail to deliver the same results *in vivo* due to lack of penetration into hypoxic areas (47, 48).

Drug penetration distances are important clinically; for example median intercapillary distances in cervix cancer have been reported to be 167μm (49). These distances were also shown to be prognostically important, likely in relation to drug delivery or hypoxia. Thus, data from this work suggest that TSLs can deliver drug to most tumor cells in such patients, considering that the 78μm drug diffusion distance is on both sides of the capillary bed. This not only provides an argument for further investigation into various nanoparticle triggers, but also allows some drugs to potentially be revisited if their efficacy has in the past been limited by drug diffusion.

Supplementary Material

Refer to Web version on PubMed Central for supplementary material.

Acknowledgments

The authors wish to thank Pavel Yarmolenko and Andrew Fontanella for their help with various aspects of the Matlab coding.

Grant Support: Funding provided by grants from the NIH/NCI CA42745-21, 22, 23, NIH/NCCAM 1F31ATT006644-01, and DOD W81XWH-09-1-0115. Financial support was also provided by the Center for Interventional Radiology, the intramural research program of the National Institutes of Health, and by a research grant from the ‘Dr. Mildred Scheel Stiftung fuer Krebsforschung (Deutsche Krebshilfe e. V.)’.

$watermark-text

$watermark-text

$watermark-text

References

1. Papahadjopoulos, D. Liposomes and Their Uses in Biology and Medicine. New York: New York Academy of Sciences; 1978.
2. Allen TM. Liposomal drug formulations. Rationale for development and what we can expect for the future. Drugs. 1998; 56:747–56. [PubMed: 9829150]
3. Wang J, Mongayt D, Torchilin VP. Polymeric micelles for delivery of poorly soluble drugs: preparation and anticancer activity in vitro of paclitaxel incorporated into mixed micelles based on poly(ethylene glycol)-lipid conjugate and positively charged lipids. J Drug Target. 2005; 13:73–80. [PubMed: 15848957]
4. Kabanov AV, Batrakova EV, Alakhov VY. Pluronic block copolymers as novel polymer therapeutics for drug and gene delivery. J Control Release. 2002; 82:189–212. [PubMed: 12175737]
5. Discher BM, Won YY, Ege DS, Lee JC, Bates FS, Discher DE, et al. Polymersomes: tough vesicles made from diblock copolymers. Science. 1999; 284:1143–6. [PubMed: 10325219]
6. Yuan F, Leunig M, Huang SK, Berk DA, Papahadjopoulos D, Jain RK. Microvascular permeability and interstitial penetration of sterically stabilized (stealth) liposomes in a human tumor xenograft. Cancer Res. 1994; 54:3352–6. [PubMed: 8012948]
7. Maeda H, Sawa T, Konno T. Mechanism of tumor-targeted delivery of macromolecular drugs, including the EPR effect in solid tumor and clinical overview of the prototype polymeric drug SMANCS. J Control Release. 2001; 74:47–61. [PubMed: 11489482]
8. Kong G, Braun RD, Dewhirst MW. Characterization of the effect of hyperthermia on nanoparticle extravasation from tumor vasculature. Cancer Res. 2001; 61:3027–32. [PubMed: 11306483]
9. Seynhaeve AL, Hoving S, Schipper D, Vermeulen CE, de Wiel-Ambagtsheer G, van Tiel ST, et al. Tumor necrosis factor alpha mediates homogeneous distribution of liposomes in murine melanoma that contributes to a better tumor response. Cancer Res. 2007; 67:9455–62. [PubMed: 17909055]
10. Tailor TD, Hanna G, Yarmolenko PS, Dreher MR, Betof AS, Nixon AB, et al. Effect of pazopanib on tumor microenvironment and liposome delivery. Mol Cancer Ther. 2010; 9 in press.
11. Dvorak HF, Nagy JA, Dvorak JT, Dvorak AM. Identification and characterization of the blood vessels of solid tumors that are leaky to circulating macromolecules. Am J Pathol. 1988; 133:95–109. [PubMed: 2459969]
12. Dreher MR, Liu W, Michelich CR, Dewhirst MW, Yuan F, Chilkoti A. Tumor vascular permeability, accumulation, and penetration of macromolecular drug carriers. J Natl Cancer Inst. 2006; 98:335–44. [PubMed: 16507830]
13. El-Kareh, AW.; Secomb, TW. Neoplasia. Vol. 2. New York, NY: 2000. A mathematical model for comparison of bolus injection, continuous infusion, and liposomal delivery of doxorubicin to tumor cells; p. 325-38.
14. Lindner LH, Eichhorn ME, Eibl H, Teichert N, Schmitt-Sody M, Issels RD, et al. Novel temperature-sensitive liposomes with prolonged circulation time. Clin Cancer Res. 2004; 10:2168–78. [PubMed: 15041738]
15. Kong G, Anyarambhatla G, Petros WP, Braun RD, Colvin OM, Needham D, et al. Efficacy of liposomes and hyperthermia in a human tumor xenograft model: Importance of triggered drug release. Cancer Res. 2000; 60:6950–7. [PubMed: 11156395]
16. Needham D, Anyarambhatla G, Kong G, Dewhirst MW. A new temperature-sensitive liposome for use with mild hyperthermia: Characterization and testing in a human tumor xenograft model. Cancer Res. 2000; 60:1197–201. [PubMed: 10728674]
17. Needham D, Dewhirst MW. The development and testing of a new temperature-sensitive drug delivery system for the treatment of solid tumors. Adv Drug Deliv Rev. 2001; 53:285–305. [PubMed: 11744173]
18. Hossann M, Wiggenhorn M, Schwerdt A, Wachholz K, Teichert N, Eibl H, et al. In vitro stability and content release properties of phosphatidylglyceroglycerol containing thermosensitive liposomes. Biochim Biophys Acta. 2007; 1768:2491–9. [PubMed: 17618599]
19. Lindner LH, Hossann M, Vogeser M, Teichert N, Wachholz K, Eibl H, et al. Dual role of hexadecylphosphocholine (miltefosine) in thermosensitive liposomes: active ingredient and mediator of drug release. J Control Release. 2008; 125:112–20. [PubMed: 18022271]

$watermark-text

$watermark-text

$watermark-text

20. Schlemmer M, Wendtner CM, Lindner L, Abdel-Rahman S, Hiddemann W, Issels RD. Thermochemotherapy in patients with extremity high-risk soft tissue sarcomas (HR-STS). Int J Hyperthermia. 2010; 26:127–35. [PubMed: 20146567]
21. Yarmolenko PS, Zhao Y, Landon C, Spasojevic I, Yuan F, Needham D, et al. Comparative effects of thermosensitive doxorubicin-containing liposomes and hyperthermia in human and murine tumours. Int J Hyperthermia. 2010; 26:485–98. [PubMed: 20597627]
22. Ponce AM, Viglianti BL, Yu D, Yarmolenko PS, Michelich CR, Woo J, et al. Magnetic resonance imaging of temperature-sensitive liposome release: drug dose painting and antitumor effects. J Natl Cancer Inst. 2007; 99:53–63. [PubMed: 17202113]
23. Weinstein JN, Magin RL, Yatvin MB, Zaharko DS. Liposomes and local hyperthermia: selective delivery of methotrexate to heated tumors. Science. 1979; 204:188–91. [PubMed: 432641]
24. Yatvin MB, Weinstein JN, Dennis WH, Blumenthal R. Design of liposomes for enhanced local release of drugs by hyperthermia. Science. 1978; 202:1290–3. [PubMed: 364652]
25. Yatvin MB, Muhlensiepen H, Porschen W, Weinstein JN, Feinendegen LE. Selective delivery of liposome-associated cis-dichlorodiammineplatinum(II) by heat and its influence on tumor drug uptake and growth. Cancer Res. 1981; 41:1602–7. [PubMed: 7194141]
26. Papenfuss HD, Gross JF, Intaglietta M, Treese FA. A transparent access chamber for the rat dorsal skin fold. Microvasc Res. 1979; 18:311–8. [PubMed: 537508]
27. Mayer LD, Bally MB, Hope MJ, Cullis PR. Uptake of antineoplastic agents into large unilamellar vesicles in response to a membrane potential. Biochim Biophys Acta. 1985; 816:294–302. [PubMed: 3839135]
28. Li L, ten Hagen TL, Schipper D, Wijnberg TM, van Rhoon GC, Eggermont AM, et al. Triggered content release from optimized stealth thermosensitive liposomes using mild hyperthermia. J Control Release. 2010; 143:274–9. [PubMed: 20074595]
29. Johansen PB. Doxorubicin pharmacokinetics after intravenous and intraperitoneal administration in the nude mouse. Cancer Chemother Pharmacol. 1981; 5:267–70. [PubMed: 7261254]
30. Poon RT, Borys N. Lyso-thermosensitive liposomal doxorubicin: a novel approach to enhance efficacy of thermal ablation of liver cancer. Expert Opin Pharmacother. 2009; 10:333–43. [PubMed: 19236203]
31. Lankelma J, Dekker H, Luque FR, Luykx S, Hoekman K, van der Valk P, et al. Doxorubicin gradients in human breast cancer. Clin Cancer Res. 1999; 5:1703–7. [PubMed: 10430072]
32. Primeau AJ, Rendon A, Hedley D, Lilge L, Tannock IF. The distribution of the anticancer drug Doxorubicin in relation to blood vessels in solid tumors. Clin Cancer Res. 2005; 11:8782–8. [PubMed: 16361566]
33. Gaber MH, Wu NZ, Hong K, Huang SK, Dewhirst MW, Papahadjopoulos D. Thermosensitive liposomes: extravasation and release of contents in tumor microvascular networks. Int J Radiat Oncol Biol Phys. 1996; 36:1177–87. [PubMed: 8985041]
34. Kong G, Braun RD, Dewhirst MW. Hyperthermia enables tumor-specific nanoparticle delivery: Effect of particle size. Cancer Res. 2000; 60:4440–5. [PubMed: 10969790]
35. Minchinton AI, Tannock IF. Drug penetration in solid tumours. Nat Rev Cancer. 2006; 6:583–92. [PubMed: 16862189]
36. Baker JH, Lindquist KE, Huxham LA, Kyle AH, Sy JT, Minchinton AI. Direct visualization of heterogeneous extravascular distribution of trastuzumab in human epidermal growth factor receptor type 2 overexpressing xenografts. Clin Cancer Res. 2008; 14:2171–9. [PubMed: 18381959]
37. Kyle AH, Huxham LA, Yeoman DM, Minchinton AI. Limited tissue penetration of taxanes: a mechanism for resistance in solid tumors. Clin Cancer Res. 2007; 13:2804–10. [PubMed: 17473214]
38. Weinstein JN, Magin RL, Cysyk RL, Zaharko DS. Treatment of solid L1210 murine tumors with local hyperthermia and temperature-sensitive liposomes containing methotrexate. Cancer Res. 1980; 40:1388–95. [PubMed: 6892792]
39. Hauck ML, LaRue SM, Petros WP, Poulson JM, Yu D, Spasojevic I, et al. Phase I trial of doxorubicin-containing low temperature sensitive liposomes in spontaneous canine tumors. Clin Cancer Res. 2006; 12:4004–10. [PubMed: 16818699]

40. Landon CD, Park JY, Needham D, Dewhirst MW. Nanoscale drug delivery and hyperthermia: the materials design and preclinical and clinical testing of low temperature-sensitive liposomes used in combination with mild hyperthermia in the treatment of local cancer. The Open Nanomedicine J. 2011; 3:38–64.
41. Celsion. ClinicalTrialsgov [Internet]. Bethesda (MD): National Library of Medicine (US); 2000. A Study of ThermoDox™ in Combination With Radiofrequency Ablation (RFA) in Primary and Metastatic Tumors of the Liver. [cited 2012 June 15]. Available from: http://www.clinicaltrials.gov/ct2/show/NCT00441376 NLM Identifier: NCT00441376
42. Celsion. ClinicalTrialsgov [Internet]. Bethesda (MD): National Library of Medicine (US); 2000. Phase 3 Study of ThermoDox With Radiofrequency Ablation (RFA) in Treatment of Hepatocellular Carcinoma (HCC). [cited 2012 June 15]. Available from: http://www.clinicaltrials.gov/ct2/show/NCT00617981 NLM Identifier: NCT00617981
43. Celsion. ClinicalTrialsgov [Internet]. Bethesda (MD): National Library of Medicine (US); 2000. Phase 1/2 Study of ThermoDox With Approved Hyperthermia in Treatment of Breast Cancer Recurrence at the Chest Wall (DIGNITY). [cited 2012 June 15]. Available from: http://www.clinicaltrials.gov/ct2/show/NCT00826085 NLM Identifier: NCT0826085
44. Dewhirst MW, Prosnitz L, Thrall D, Prescott D, Clegg S, Charles C, et al. Hyperthermic treatment of malignant diseases: current status and a view toward the future. Seminars in oncology. 1997; 24:616–25. [PubMed: 9422258]
45. van der Zee J, Vujaskovic Z, Kondo M, Sugahara T. The Kadota Fund International Forum 2004--clinical group consensus. Int J Hyperthermia. 2008; 24:111–22. [PubMed: 18283588]
46. Issels RD, Lindner LH, Verweij J, Wust P, Reichardt P, Schem BC, et al. Neo-adjuvant chemotherapy alone or with regional hyperthermia for localised high-risk soft-tissue sarcoma: a randomised phase 3 multicentre study. Lancet Oncol. 2010; 11:561–70. [PubMed: 20434400]
47. Cardenas-Navia LI, Secomb TW, Dewhirst MW. Effects of fluctuating oxygenation on tirapazamine efficacy: Theoretical predictions. Int J Radiat Oncol Biol Phys. 2007; 67:581–6. [PubMed: 17236974]
48. Hicks KO, Pruijn FB, Secomb TW, Hay MP, Hsu R, Brown JM, et al. Use of three-dimensional tissue cultures to model extravascular transport and predict in vivo activity of hypoxia-targeted anticancer drugs. J Natl Cancer Inst. 2006; 98:1118–28. [PubMed: 16912264]
49. West CM, Cooper RA, Loncaster JA, Wilks DP, Bromley M. Tumor vascularity: a histological measure of angiogenesis and hypoxia. Cancer Res. 2001; 61:2907–10. [PubMed: 11306466]

$watermark-text
$watermark-text
$watermark-text

$watermark-text
$watermark-text
$watermark-text

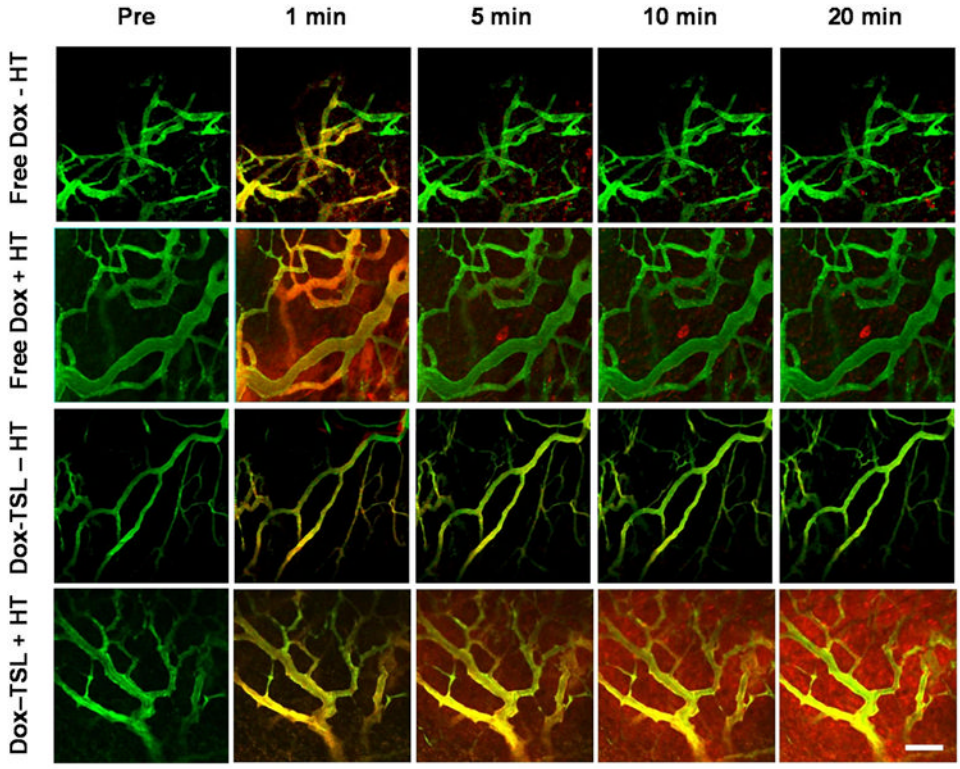

Figure 1. Tumor uptake of doxorubicin as a function of time

Time sequence images of fluorescein-labeled dextran inside blood vessels (green) and doxorubicin (red). The top two rows show free drug delivery over time ± heat. Free drug injection results in drug delivery to the interstitium that is quickly reabsorbed into the vasculature within 5min, with few cells taking up large amounts of drug. The bottom two panels display fluorescein-labeled liposomes (green) and doxorubicin (red). In contrast to free drug, heating TSLs results in continuous drug delivery to tissue; dramatic uptake by cells is seen far from vessels, by 20min. Additionally, drug is delivered without extravasation by the liposomes (lack of yellow color in interstitial space), indicative of *intravascular* release. The Dox-TSL - HT panel illustrates that TSLs do not release appreciable amounts of drug into tissue when not heated. Scale bar = 100μm.

$watermark-text
$watermark-text
$watermark-text

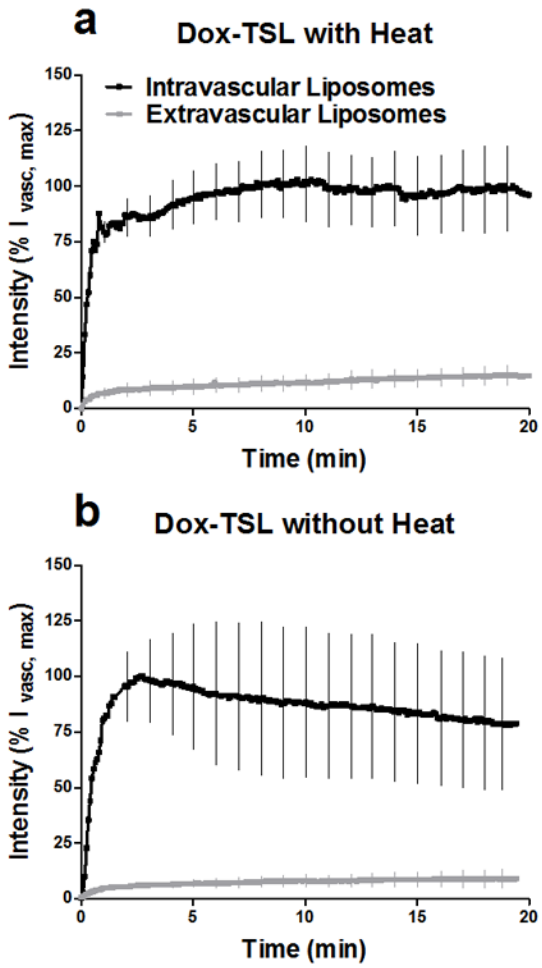

Figure 2. Liposome intravascular kinetics and extravasation over time

Over the timecourse of drug delivery, liposomes stay inside the vasculature, indicating intravascular drug release. Liposome fluorescence is portrayed as a percentage of the peak intravascular fluorescein fluorescence (%$I_{vasc,max}$). (**a**) liposomes delivered to a heated-tumor (n=6). (**b**) liposomes delivered to an unheated-tumor (n=4). Data is expressed as means and SD.

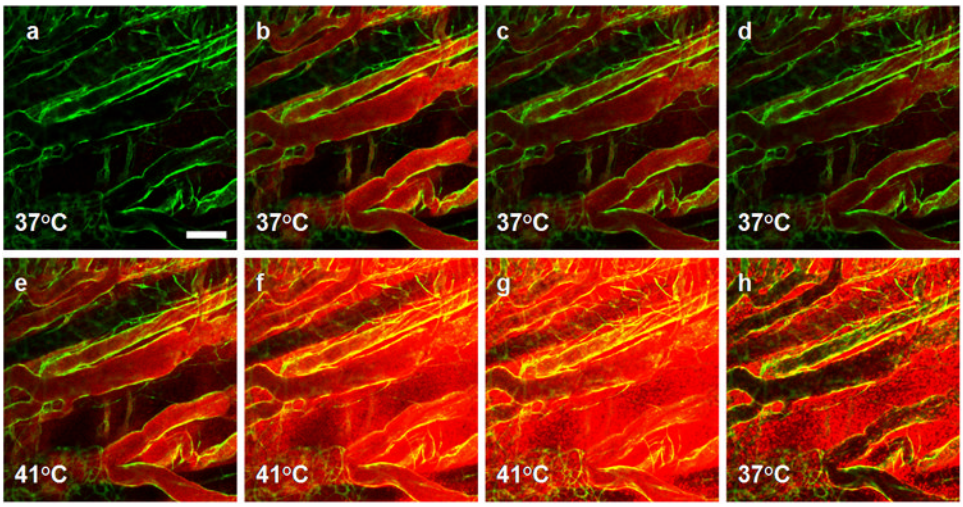

Figure 3. Intravascular release of doxorubicin

In the eNOS-GFP mouse model, GFP signal (green) is restricted to the endothelial cell layer. **(a)** Background vessels prior to injection. **(b)** Immediately after intravenous injection of Dox-TSL into tissue at 37°C, doxorubicin distribution becomes apparent by localized fluorescence (red) in the intravascular space (bolus phase, 0.5min). **(c and d)** 2-5min post-injection at 37°C, the drug fluorescence is still confined to the vascular space although the signal intensity is reduced, indicating a loss of liposomes from the blood stream. **(e)** 1min after the onset of heat treatment at 41°C, the intravascular drug signal increases due to intravascular release of doxorubicin and dequenching effects as the drug leaves the liposome interior. **(f)** After 5min of heating, extravascular doxorubicin accumulation becomes visible. **(g)** Drug accumulation increases in time with heating, and reaches a maximum at 15min into heating. **(h)** 10min after stopping heat most unbound free doxorubicin is washed out of the bloodstream and doxorubicin-stained nuclei remain fluorescent. Scale bar = 100μm.

$watermark-text
$watermark-text
$watermark-text

$watermark-text
$watermark-text
$watermark-text

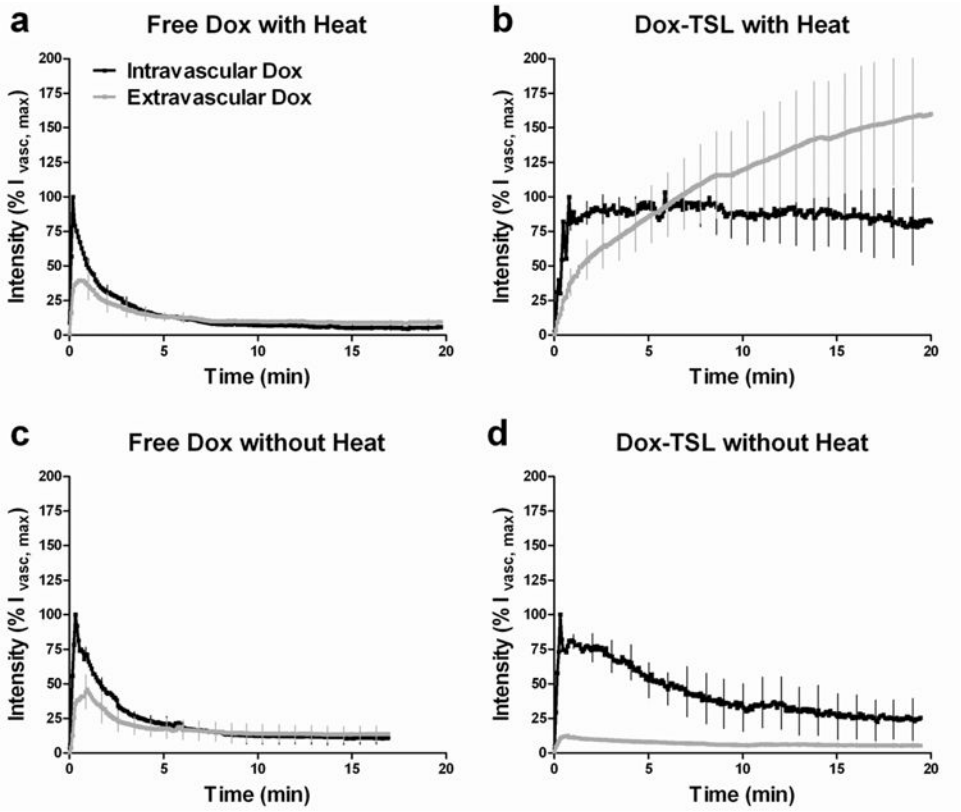

Figure 4. Vascular pharmacokinetics and extravascular accumulation of doxorubicin in tumor tissue over time

Doxorubicin accumulation inside the vasculature and in the extravascular space is displayed as a percentage of the peak intravascular fluorescence (%$I_{vasc,max}$). (**a**) Free doxorubicin administration +heat (n=5). (**b**) Doxorubicin compartmentalization after Dox-TSL injection into a heated tumor (n=6). (**c**) Free doxorubicin administration without heat (n=5). (**d**) Doxorubicin compartmentalization after Dox-TSL injection into an unheated tumor (n=4). Doxorubicin accumulation in the tumor tissue following free drug administration peaks within the first minute. Drug levels then begin to decline, with residual extravascular doxorubicin at around 10% of the initial injected amount (9.6% +/- 2.0 heated, 13.7% +/- 5.7% non-heated). In contrast, doxorubicin levels continue to increase when delivered with Dox-TSL+heat. At 20min into treatment, drug is still accumulating, with extravascular levels at 160% +/- 47% of the initial injected drug amount. Without heat, the nanoparticles shield drug from tissue, and doxorubicin accumulation levels are minimal (5.4% +/- 1.9%), maintaining the toxicity benefits of traditional nanoparticle drug delivery. Data is expressed as means and SD.

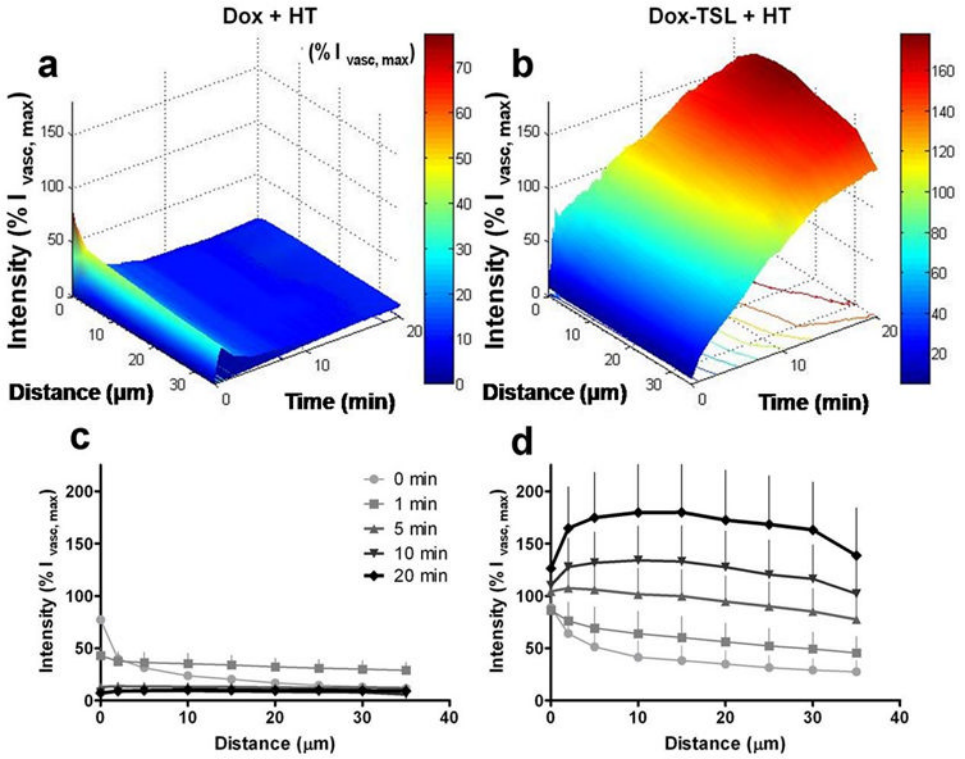

Figure 5. Drug penetration into tumor tissue from vessels through time

Doxorubicin penetration into the extravascular space is displayed as a percentage of the peak intravascular fluorescence ($\%I_{vasc,max}$) through time. Figures (**a**) and (**b**) display differences in drug accumulation with both time and penetration distance. Figures (**c**) and (**d**) further display this data at specified time points. Time 0min corresponds to the time of peak intravascular concentration, with the zero distance defined as the space immediately adjacent to the vascular compartment. (**a**/**c**) Free doxorubicin administration +heat (n=5). Free drug exhibits characteristic exponential decline in drug levels with vasculature, but within minutes most of the drug is reabsorbed into the bloodstream. (**b**/**d**) Doxorubicin compartmentalization after Dox-TSL injection into a heated tumor (n=6). In contrast with free drug injection, doxorubicin delivered with Dox-TSL results in an alteration of penetration characteristics, with continual buildup of drug into the interstitial space. Data is expressed as means and SD.

$watermark-text
$watermark-text
$watermark-text

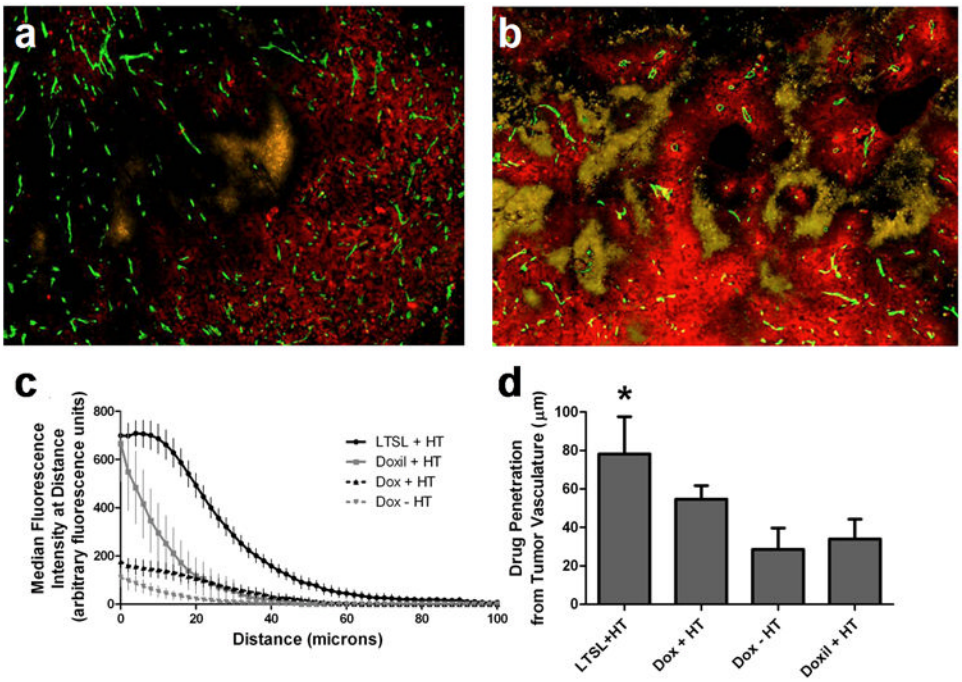

Figure 6. Histologic assessment of drug penetration from vessels in a flank tumor model

Figures (**a** and **b**) are histology images following free doxorubicin + HT (**a**) and Dox-TSL + HT (**b**) treatments, with drug (red), vessels stained with CD31 (green), and EF5 hypoxia marker (yellow) (while these images vary in extent of hypoxia, there was no statistical difference in the extent of hypoxia across all tumors). Figure (**c**) expresses drug levels as median fluorescence intensity at distances out to 100μm from the nearest blood vessel. Dox-TSL delivers more drug at all distances from vessels compared to Doxil™ and free doxorubicin ± heat. At the distance Dox-TSL levels start to fall, Doxil™ levels are less than half that of Dox-TSL and have already fallen to approximately 1/3 of their maximal concentration close to blood vessels. Figure (**d**) shows the maximum drug penetration from tumor vasculature vs. treatment group and demonstrates that drug delivered with Dox-TSL penetrates twice as far as with traditional Doxil™ liposomes (78 vs. 34μm, p-value = 0.0106). Data are expressed as medians (**c**) and means (**d**) with SD.

$watermark-text
$watermark-text
$watermark-text